Journal of Alzheimer's Disease 54 (2016) 79–88
DOI 10.3233/JAD-160253
IOS Press

Biofunctionalized Silica Nanoparticles: Standards in Amyloid-β Oligomer-Based Diagnosis of Alzheimer's Disease

Maren Hülsemann[a,1], Christian Zafiu[a], Katja Kühbach[a], Nicole Lühmann[b], Yvonne Herrmann[a], Luriano Peters[a], Christina Linnartz[a], Johannes Willbold[a], Kateryna Kravchenko[a], Andreas Kulawik[a], Sabine Willbold[b], Oliver Bannach[a,c] and Dieter Willbold[a,c,*]
[a]*Forschungszentrum Jülich, ICS-6, Institut für Strukturbiochemie, Jülich, Germany*
[b]*Forschungszentrum Jülich, ZEA-3, Zentralinstitut für Engineering, Elektronik und Analytik, Jülich, Germany*
[c]*Heinrich-Heine-Universität Düsseldorf, Institut für Physikalische Biologie, Düsseldorf, Germany*

Handling Associate Editor: Piotr Lewczuk

Accepted 23 May 2016

Abstract. Amyloid-β (Aβ) oligomers represent a promising biomarker for the early diagnosis of Alzheimer's disease (AD). However, state-of-the-art methods for immunodetection of Aβ oligomers in body fluids show a large variability and lack a reliable and stable standard that enables the reproducible quantitation of Aβ oligomers. At present, the only available standard applied in these assays is based on a random aggregation process of synthetic Aβ and has neither a defined size nor a known number of epitopes. In this report, we generated a highly stable standard in the size range of native Aβ oligomers that exposes a defined number of epitopes. The standard consists of a silica nanoparticle (SiNaP), which is functionalized with Aβ peptides on its surface (Aβ-SiNaP). The different steps of Aβ-SiNaP synthesis were followed by microscopic, spectroscopic and biochemical analyses. To investigate the performance of Aβ-SiNaPs as an appropriate standard in Aβ oligomer immunodetection, Aβ-SiNaPs were diluted in cerebrospinal fluid and quantified down to a concentration of 10 fM in the sFIDA (surface-based fluorescence intensity distribution analysis) assay. This detection limit corresponds to an Aβ concentration of 1.9 ng l^{-1} and lies in the sensitivity range of currently applied diagnostic tools based on Aβ oligomer quantitation. Thus, we developed a highly stable and well-characterized standard for the application in Aβ oligomer immunodetection assays that finally allows the reproducible quantitation of Aβ oligomers down to single molecule level and provides a fundamental improvement for the worldwide standardization process of diagnostic methods in AD research.

Keywords: Alzheimer's disease diagnosis, Aβ oligomer standards, assay standardization, biofunctionalized nanoparticles

INTRODUCTION

Alzheimer's disease (AD) is the most common form of dementia, affecting more than 33 million people worldwide and the case number is expected to triple over the next four decades [1, 2]. AD represents a multifactorial disorder with a yet poorly understood pathogenesis, which makes its early and accurate diagnosis a difficult challenge [3]. Currently, there is no causal therapy available and a reliable diagnosis can only be achieved by post mortem analysis of brain samples.

The 'amyloid cascade' hypothesis is widely accepted to explain development and progression of AD. It mainly postulates an imbalance between

[1]Current address: Albert Einstein College of Medicine, Institute of Anatomy and Structural Biology, Laboratory of Molecular and Cellular Biophysics, New York City, USA.

*Correspondence to: Prof. Dr. Dieter Willbold, ICS-6, Institut für Strukturbiochemie, Forschungszentrum Jülich, 52428 Jülich, Germany. Tel.: +49 2461 61 2100; Fax: +49 2461 61 2023; E-mail: d.willbold@fz-juelich.de.

expression and clearance of amyloid-β (Aβ) peptides in the brain. The Aβ overload favors Aβ aggregation, ultimately inducing neuronal and synaptic degeneration and leading to dementia [4]. More recent data suggest that soluble oligomers of Aβ, in particular, directly correlate with disease severity [5, 6]. Thus, Aβ oligomers represent a popular target in drug development as well as a promising biomarker candidate for both early diagnosis of AD and therapy monitoring, respectively. A broad range of diagnostic methods for detection and quantitation of Aβ oligomers is currently applied or under evaluation. The concentration of Aβ oligomers in human body fluids is commonly assayed by ELISA methods, using capture antibodies and detection antibodies that bind to the same or overlapping epitopes, or by application of oligomer-specific antibodies [7–14].

We previously described the surface-based fluorescence intensity distribution analysis (sFIDA) technology as a highly oligomer-specific detection and quantitation method for the early diagnosis of AD [15, 16].

In sFIDA, a glass surface is covalently coated with anti-Aβ capture antibodies (Nab228, Epitope $Aβ_{1–11}$) which immobilize Aβ species from the sample. In the next step, Aβ oligomers are labeled by at least two different fluorophore-coupled anti-Aβ antibodies. Since all three applied antibodies recognize overlapping epitopes in the N-terminal part of Aβ, only oligomeric structures can be immobilized and bound by both detection antibodies at the same time, which makes the sFIDA technique insensitive against Aβ monomers. The use of different antibodies with affinities to a pan-epitope (6E10-488, Epitope $Aβ_{3–8}$ and IC16-633, Epitope $Aβ_{1–8}$) enhances the specificity of the assay, since only co-localized signals are counted but not signals caused by cross-reactivity of the individual antibodies. Finally, the chip surface is imaged by dual-color TIRF microscopy. After application of an intensity threshold the number of colocalized pixels from both channels is counted and correlates with the number of oligomers in the samples and is referred to as sFIDA readout.

While assays quantitating total Aβ can readily be calibrated with synthetic Aβ monomers, it is very difficult to establish standards for oligomer-based diagnostic tests. Furthermore, there are large variations in Aβ oligomer measurements among and within laboratories [17].

Therefore the development of a reliable oligomer standard is highly needed, since the readouts of these quantitation tests are dependent on calibration curves of standard molecules. The use of oligomers or aggregates from synthetic Aβ is limited, as these structures are metastable, heterogeneous and in dynamic equilibrium with other assembly states, and hence do not have defined sizes or consistent molecular weights. Additionally, oligomers from synthetic Aβ are prone to further aggregation and susceptible to freeze/thaw cycles, making long-term storage and constant performance, as pre-requirements for any standard, impossible.

In this work we present a novel concept for the synthesis of Aβ oligomer standards, suitable for the application in Aβ oligomer-specific quantitation assays. The core and size-determining component of the standard is a SiNaP, which can be adjusted to any size required with nearly a monodisperse size distribution [18, 19]. SiNaPs are chemically inert, non-toxic, easy to modify and stable over months. These features make SiNaPs a highly favored substructure in the design of the standard. To simulate characteristics of a native oligomer, the size of the SiNaPs was tuned to the described size range of native oligomers of 3 to 20 nm [20–22]. The surface of the SiNaPs was functionalized, activated and finally coated with $Aβ_{42}$ peptides. These biofunctionalized Aβ-SiNaPs exhibit a defined number of Aβ epitopes on the surface and allow their application in quantitative oligomer-based detection assays.

To our knowledge no other available Aβ oligomer standard presents as defined characteristics as our standard, which will therefore have a major impact on the accurate and reproducible quantitation of Aβ oligomers in human samples. Aβ-SiNaPs are a helpful accomplishment for the urgently needed standardization process between different operators, laboratories, and clinical studies in AD research worldwide [17].

MATERIAL AND METHODS

Synthesis of SiNaPs according to the Stöber process

200 ml absolute ethanol (VWR, Darmstadt, Germany), 2.7 ml water, and 4.49 ml ammonia solution (25%, Carl Roth, Karlsruhe, Germany) were vigorously stirred in a round bottom flask. After 5 min 4.43 ml TEOS (tetraethylorthosilicate, Aldrich Chemistry, St. Louis, USA) were added and the solution was stirred further for 2 days at room temperature. The resulting SiNaPs were dialyzed (MWCO

3,500, Tubing Spectral Por7 Dialysis Membrane, Spektrum Laboratories, Rancho Dominguez, CA, USA) against fivefold the volume of ethanol for 2 days to remove non-reacted chemicals and the catalysts. The SiNaPs reached a concentration of about 10 g l^{-1} and were stored at 4°C in ethanol until further usage.

Particle characterization by TEM, XPS, and FTIR

The morphology of the SiNaPs was determined by transmission electron microscopy (TEM). TEM images were recorded using a Zeiss Libra 120 Transmission Electron Microscope (Carl Zeiss AG, Jena, Germany). The copper grids (S160, Plano GmbH, Wetzlar, Germany) were prepared without staining by placing a 5 µl drop of SiNaPs (1 to 0.1 mg ml^{-1}) in ethanol on the carbon film of the grid and letting it dry at room temperature for at least 3 h before measurement.

The different SiNaP functionalization steps were monitored by Fourier transformed Infrared Spectroscopy (FTIR) and X-ray photoelectron spectroscopy (XPS). FTIR spectra were obtained by a Bruker Tensor 27 (Bruker Optik GmbH, Ettlingen, Germany) equipped with an attenuated total reflection (ATR) unit (Golden Gate, diamond crystal, Specac Ltd, UK). A film of the particles was prepared by drop casting dispersion in ethanol onto the diamond crystal. The spectra were collected with 128 scans at resolution of 4 cm^{-1} after the solvent signals in the IR spectrum vanished. The beam path was purged with argon during the measurements.

XPS spectra were obtained by a PHI 5000 VersaProbe II emitting monochromatic Al-kα radiation at an angle of 46°. A film of particles was drop casted on glass slides and the solvent was evaporated over night before measurement. Spectra were obtained from three individual positions on the glass slides.

Calculations and assumptions

After size determination of the SiNaPs by TEM micrographs, the particle surface was calculated, assuming a spherical surface. The molecular weight of the SiNaP was calculated assuming an average density of 1.85 g cm^{-3} [23]. The concentration of the SiNaP solution was determined gravimetrically in triplicate and the mean concentration of the SiNaP was calculated after every functionalization step, so that chemicals for further functionalization steps were added accordingly.

The number of potential binding sites on the SiNaP surface was determined under the assumption that one APTES molecule occupies a surface of 0.6 nm^2 [24].

Synthesis of amino-functionalized SiNaPs

Amino-functionalized SiNaP were prepared via silanization with APTES ((3-aminopropyl) triethoxysilane, Sigma-Aldrich, St. Louis, USA). A 5-fold molar excess of APTES in relation to the number of potential binding sites on the particle surface was added to the SiNaPs in ethanol. The dispersion was sonicated for 10 min and incubated overnight on a shaker at ambient temperature. The resulting amino-functionalized SiNaPs were centrifuged (5,000 × *g*, 2 h) and the resulting pellet was dispersed in ethanol by sonication for 15 min. This washing step was repeated three times.

Synthesis of carboxylated SiNaPs

A pellet containing amino-functionalized SiNaP was re-dispersed in 0.1 M succinic anhydride (Aldrich Chemistry, St. Louis, USA) in DMF (AppliChem, Darmstadt, Germany) under argon atmosphere and stirred overnight. The resulting carboxylated SiNaPs were alternately washed with water and ethanol for three times by centrifugation (5,000 × *g*, 2 h) and pellet resuspension.

Peptide coupling to the SiNaP surface

The carboxylated SiNaPs (cSiNaP) were re-dispersed in 10 mM MES buffer, pH 5.7 (Sigma Aldrich, St. Louis, USA) and were activated by EDC (1-ethyl-3-(3-dimethylaminopropyl) carbodiimide, Fluka, Sigma Aldrich, St. Louis, USA) and NHS (N-hydroxysuccinimide, Aldrich Chemistry, St. Louis, USA). The chemicals were added to the particle solution in a 16-fold and 4-fold molar excess respectively, compared to the potentially bound APTES molecules, and the mixture was sonicated for 10 min. The dispersion was centrifuged for 1 h at 10,000 × *g* and the pellet was re-dissolved in 10 mM MES buffer (pH 5.7) again. The washing procedure was repeated once before the NHS-ester activated SiNaPs were added to the peptides.

The concentration of the pre-activated SiNaPs was gravimetrically determined and the theoretical number of NHS ester groups on the SiNaP surface was

calculated. The pre-activated SiNaPs were added to the peptide resulting in a 1 : 1 ratio of potential binding sites (i.e., NHS ester groups) versus peptides, whereas a complete binding of all peptides to the particle surface cannot be expected due to the size of the peptide. The Aβ monomer has a hydrodynamic radius of 0.9 nm ± 0.1 nm [25] which would allow a maximum surface coverage of 645 peptides per SiNaP.

The dispersion of SiNaPs and peptide was sonicated for 20 min and incubated under shaking overnight. On the next day the Aβ-coated SiNaPs were centrifuged again and the pellet was re-dispersed in aqueous 50% HFIP solution (hexafluoroisopropanol, Merck, Darmstadt, Germany) to remove non-covalently bound protein. The SiNaPs were sonicated in HFIP for 5 min, followed by centrifugation (5,000 × *g*, 1 h). The last washing step was performed in water and the peptide-coated SiNaPs were stored in water at 4°C until further usage.

Peptide preparation

1 mg $A\beta_{42}$ lyophilisates (Bachem, Bubendorf, Switzerland) were dissolved in 500 µl HFIP and incubated overnight. On the next day another 500 µl HFIP were added to the peptide solution and 200–500 µl (1 µg µl^{-1}) Aliquots were prepared and the solvent was evaporated. The dry aliquots were frozen at –20°C until further usage.

Determination of the peptide concentration by BCA assay

The Kit Extra Sense BCA Assay Protein Assay Kit (BioVision Incorporated, Catolog number K814-2500, *Microplate Procedure*) was used to determine the peptide load on the SiNaPs surface. Therefore 150 µl of $A\beta_{42}$ SiNaP were mixed with 150 µl 6 M Urea (Urea crystalline, AppliChem, Darmstadt, Germany) and the solution was incubated at 60°C for 30 min. 150 µl of working solution was added and the mixture was heated at 60°C for 1 h, before the absorption at 562 nm was measured by UV/VIS spectrometry. The protein concentration was calculated according to Beer-Lambert equation.

sFIDA protocol

Custom-made 96 well plates were manufactured by gluing a 170 µm thick glass bottom (Menzel Gläser, Thermo Fisher Scientific, MS, USA) to a 0.5 cm glass plate which was perforated with 96 holes. Prior to use, plates were cleaned with ethanol and water. For further purification and hydroxylation of the glass surface the wells were treated with 5 M NaOH (Karl Roth, Karlsruhe, Germany) for 3 h. Further washing with water and drying of the plate at 90°C was followed by H_2O-Plasma treatment (Diener electronics GmbH, Ebhausen, Germany). Afterwards a desiccator was flushed with argon gas and two trays containing 1 ml of APTES and 200 µl of TEA (triethylamine, Sigma Aldrich, St. Louis, USA), respectively, were added to the chamber. The 96 well full glass plate was placed into the desiccator with the wells facing the filled trays. The chamber was flushed with argon again and vapor deposition of APTES on the glass surface was performed overnight. Next day the chemicals were removed and the desiccator was again flushed with argon and the plate got cured inside for at least 4 h (storage possible up to one week).

Carboxyl groups of 20 mg ml^{-1} carboxymethyldextrane (CMD, Sigma Aldrich, St. Louis, USA) in water were activated by 200 mM EDC and 50 mM NHS for 0.5 h under shaking. Afterwards the mixture was added to the amino-functionalized glass plates to establish amide bonds between the CMD network and the glass surface. After 1.5 h the CMD solution was removed and the wells were washed with water three times.

The remaining carboxyl groups of the bound CMD were activated by 200 mM EDC and 50 mM NHS in water again for 0.5 h. After removing EDC/NHS and performing two washing steps with water, 1 mg l^{-1} anti-Aβ capture antibody (Nab 228, epitope $A\beta_{1-11}$, Sigma Aldrich, St. Louis, USA) in PBS was added to the wells. The incubation for 1.5 h led to the covalent binding of the capture antibody to the surface.

After removing the antibody solution the remaining active NHS-ester groups on the functionalized surface were quenched by 0.1 M ethanolamine hydrochloride (Sigma Aldrich, St. Louis, USA) in Tris-buffered saline, pH 7.4 (TBS). The solution was removed after 30 min and the wells were washed with TBS three times. Until sample application the plates were stored in TBS.

15 µl of samples were applied to the plate in triplicates and incubated overnight on the capture-antibody coated glass surface. Afterwards the wells were washed once with TBS-T (TBS supplemented with 0.05% Tween-20) and twice with TBS. In the next step, 1.25 mg/l of two fluorescence-labeled anti-Aβ antibodies IC16-Alexa 633 and 6E10-ATTO 488 (6E10: epitope $A\beta_{3-8}$, Covance, Princeton, USA;

dye: ATTO-Tec, Siegen, Germany) were added to the wells and incubated for 2 h. mAB IC16 (epitope $A\beta_{1-8}$) was kindly provided by the groups of Prof. Carsten Korth and Prof. Sascha Weggen, Heinrich Heine University Düsseldorf Medical School and labeled with Alexa 633 dye according to the manufactures instructions (Life Technologies, Carlsbad, USA). Finally, the wells were washed twice with TBS-T and twice with TBS. Prior to TIRF microscopy the wells were filled with water and sealed with a plastic foil.

Application of Aβ-SiNaPs in sFIDA

Aβ-SiNaPs were stored in water at 4°C until use. For sFIDA analysis, Aβ-SiNaPs were serially diluted in water and human AD-negative CSF (biochemed, Winchester, USA) to concentrations ranging from 100 pM down to 10 fM and analyzed by sFIDA in threefold determination.

Data acquisition

The surface of the sFIDA well plates was imaged by total internal reflection fluorescence (TIRF) microscopy (AM TIRF MC Leica TIRF microscope, Leica Microsystems, Wetzlar, Germany). The measurement was performed by the Leica Matrix screener software using a 100 × objective lens (1.47 oil CORR TIRF Leica), which enabled the detection of surface-near fluorescence. For each well, 25 images (112 × 112 μm, 1000 × 1000 pixels, 200 nm distance between the scan areas, 14 bit) were taken in channel 0 (Ex/Em 635/705 nm), and channel 1 (Ex/Em 488/525 nm), detecting IC16-Alexa 633 and 6E10-ATTO 488 respectively. Microscope settings of gain, laser power and exposure time were adjusted in a way that the intensity histogram still showed a detectable fluorescence signal for the lowest standard concentration. The microscope settings included a gain between 800 and 1000, a laser power of 100% and an exposure time between 1 and 1.8 s.

Data analysis

After data acquisition at the TIRF microscope the images were exported as tiff files and analyzed with a self-developed software designated sFIDAta. The performed image analysis was applied only to the central 700 × 700 pixels of each image. By this procedure, the border regions of all images, which are not uniformly illuminated, were excluded from the analysis. The software performed a separated histogram analysis for each channel and each SiNaP concentration. To exclude the background signal, intensity cutoffs were determined for each channel. Since the background signal can differ between different matrices (water or CSF), cutoffs were calculated individually for each matrix. The cutoff is defined as an intensity threshold that leaves 0.1% of the total pixel number in the images from the blank control measurement (i.e., 1,000 pixels out of a million pixels). Finally, images from both channels were merged and the number of colocalized pixels above the determined cutoffs was counted for each well. The mean number of colocalized pixels from the images of each concentration is referred to as 'sFIDA readout'.

RESULTS

Synthesis of SiNaPs

SiNaPs were produced as the core component of the standard. Synthesis of the SiNaPs was performed via the Stöber process, which describes a condensation reaction of tetraethylorthosilicate (TEOS) to a siloxane polymer network in the presence of water and ammonia, resulting in nearly monodisperse SiNaPs [18]. Since the diameter of a native oligomer is in the range of 3 to 20 nm, we aimed to synthesize the SiNaP core in an according size range. To determine the size and morphology of the obtained SiNaPs, transmission electron micrographs were recorded. Figure 1 shows SiNaPs with a mean diameter of 24 ± 4.6 nm exhibiting a rather polyhedral shape. It has been previously reported that the shape of very small SiNaPs (<50 nm) is not spherical due to the mechanism of particle formation [18, 23].

Synthesis strategy of biofunctionalized SiNaPs

For biofunctionalization of SiNaPs, three functionalization steps were performed as described in Fig. 2a-e. After synthesis of SiNaPs via the Stöber process (Fig. 2a) a primary amine group was introduced to the SiNaP surface by silanization with APTES (3-(aminopropyl)triethoxysilane) (Fig. 2b, aminated SiNaP = aSiNaP). In the next step aSiNaPs were transferred to a solution of succinic anhydride in DMF (dimethylformamide) under dry conditions. The amine group on the SiNaP surface attacked the succinic anhydride which led to a ring-opening of the anhydride, the formation of an amide bond and

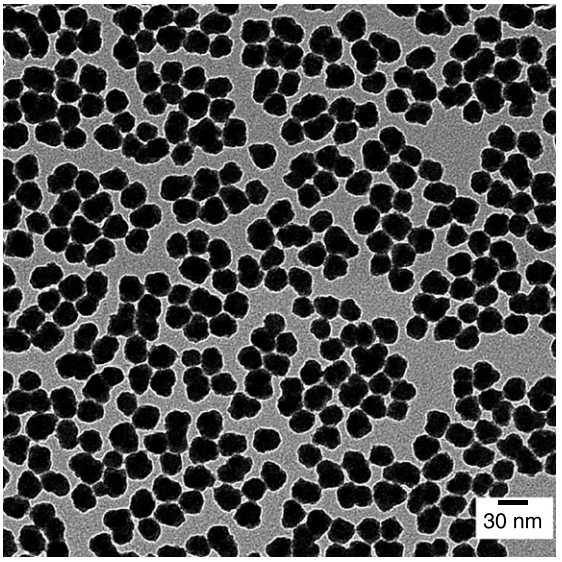

Fig. 1. Transmission electron micrographs of bare SiNaPs. A mean Feret diameter of 24 ± 4.6 nm was calculated from at least 250 SiNaPs.

the exposure of free carboxyl groups on the SiNaP surface (Fig. 2c, carboxylated SiNaP = cSiNaP) [26].

The activation of the exposed carboxyl groups by EDC/NHS (1-ethyl-3-(3-dimethylaminopropyl) carbodiimide / N-hydroxysuccinimide) resulted in the formation of NHS ester groups (Fig. 2d, activated SiNaP) which could react with primary amine groups of chosen biomolecules (Fig. 2e) and led to their covalent binding on the SiNaP surface.

The successful modifications of the SiNaP surface was monitored by XPS and attenuated total reflection Fourier transform infrared spectroscopy (ATR-FTIR). Figure 3a shows the atomic composition of SiNaP and aSiNaP obtained from XPS spectra. Both nanoparticles exhibited high levels of oxygen and silicon atoms which originated from the dense silica core of the materials. Elevated levels of carbon and nitrogen in aSiNaP spectra suggest the surface modification with APTES as these signals were absent in the case of unmodified SiNaP.

Figure 3b shows full range FTIR spectra of different modification steps of SiNaP and a predominant band ranging from 1300 and 1000 cm^{-1} which corresponds to the Si-O and Si-OH bonds of amorphous silicate material. Another common feature of the spectra is a broad band between 3800 and 2700 cm^{-1} (Fig. 3c) which represents the O-H vibrations within the SiNaP core.

Unmodified SiNaP show two characteristic bands, one at 3650 cm^{-1} (free -O-H strech) and in Fig. 3d

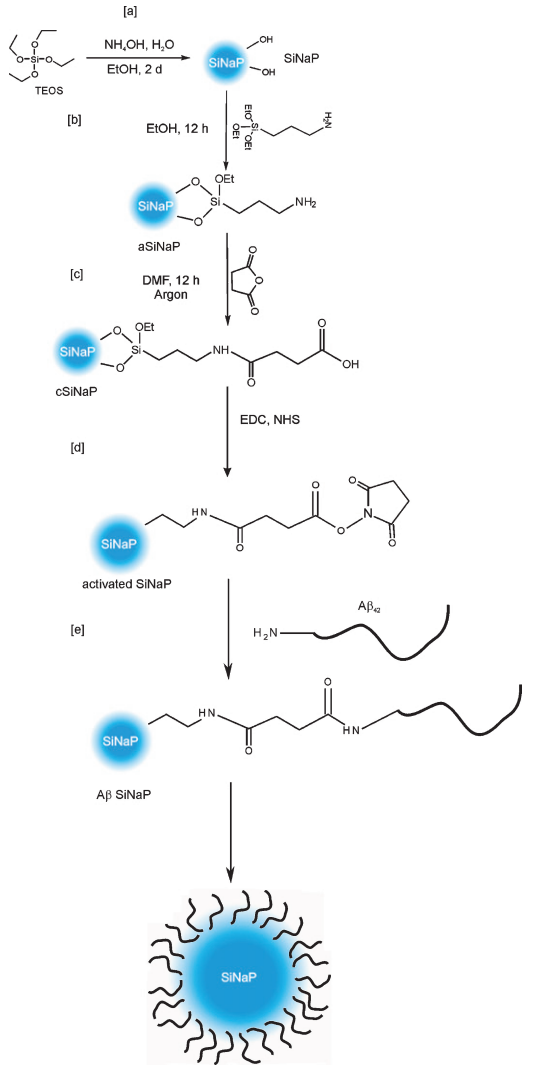

Fig. 2. Synthesis strategy of biofunctionalized SiNaPs. a) Stoeber synthesis of SiNaPs was followed by (b) silanization of the SiNaP surface with APTES (aSiNaP). c) Primary amines reacted with succinic anhydride via a nucleophilic addition and led to the introduction of carboxy functions on the SiNaP surface (cSiNaP). d) Carboxy groups became activated to reactive NHS esters by EDC/NHS (activated SiNaP) which (e) reacted with amine groups of biomolecules, such as Aβ peptides and led to their covalent binding on the SiNaP surface.

at 1650 cm^{-1} (-O-H bend) that represent the -O-H surface functionalities. Furthermore, the spectrum consisted of a broad band at 1450 cm^{-1} which could be assigned to carbonate anions as an insertion product of CO_2 into the silanol group of the silica surface.

After exposing SiNaP to APTES CH_2 scissoring bands at 1395 and 1445 cm^{-1} were observed together with C-H stretching bands between 2900 and 2980 cm^{-1}. In addition a weak band at 1620 cm^{-1}

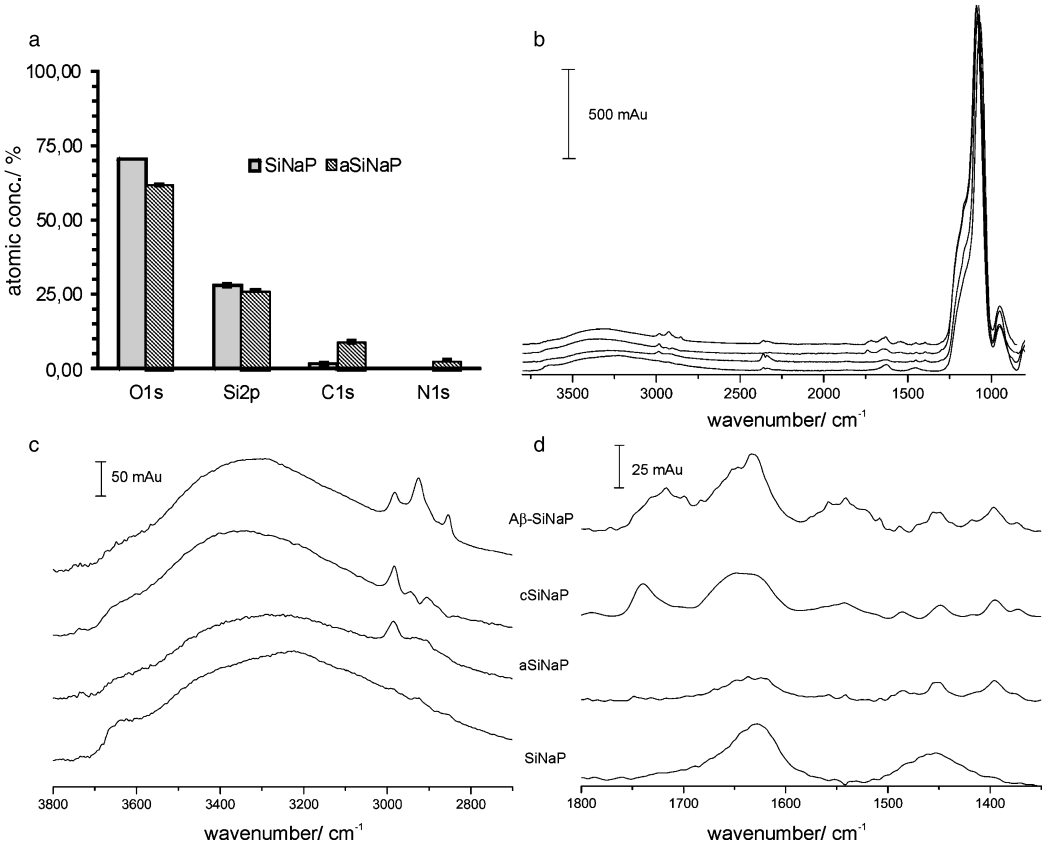

Fig. 3. a) XPS data analysis of SiNaP (grey) and aSiNaP (striped). b) ATR-FTIR spectra of different SiNaP functionalization steps. SiNaP: unmodified SiNaP, aSiNaP: aminated SiNaP functionalized with APTES, cSiNaP: carboxylated SiNaP functionalized with succinic anhydride; Aβ-SiNaP: SiNaP coated with Aβ. c) Expanded spectra from (b) in the range of 2700 – 3800 cm^{-1}. d) Expanded spectra from (b) in the range of 1300 – 1800 cm^{-1}.

represents the -N-H surface functionality which was also observed by XPS (Fig. 3a).

The modification of the SiNaPs by succinic acid was confirmed in the FTIR spectra by the appearance of two new bands at 1655 and 1723 cm^{-1} (COOH and COO^- vibrations respectively). The band at 1655 cm^{-1} overlaps with an additional one at 1630 cm^{-1}, which is typical for the amide I vibration.

Bioconjugation of SiNaPs with synthetic Aβ

The bioconjugation of SiNaPs with chosen biomolecules was enabled by previous functionalization and activation of the surfaces of SiNaPs by EDC/NHS treatment and the formation of NHS ester groups as reactive intermediates (Fig. 2d, e). The NHS esters on the surfaces of SiNaPs formed amide bonds with the exposed lysine residues of $A\beta_{42}$ at position 16 and/or 28 and led to coating of SiNaPs with Aβ peptides. An additional binding site is the N-terminus of the peptide, which we consider less reactive for the coupling reaction due to its vicinity to acidic amino acids and steric restraints. The successful attachment of $A\beta_{42}$ to the particles was demonstrated by FTIR (Fig. 3). Not only the bands assigned to CH_2 stretching vibrations (2925 cm^{-1} and 2855 cm^{-1}) showed an increased intensity for the peptide coated SiNaPs, but also the signals between 1580 and 1750 cm^{-1}. The increase of the band at 1720 cm^{-1} (COOH) appeared due to the presence of additional carboxyl groups by the amino acids of $A\beta_{42}$. Whereas the amide I vibration of the COOH-terminated SiNaPs was only visible as a shoulder which was increased to a maximum for the $A\beta_{42}$ functionalized SiNaPs. A new band positioned at 1542 cm^{-1} could be assigned to the amide II vibration of the peptide as well. Peptide quantitation by BCA assay revealed an $A\beta_{42}$ concentration of 24 μg ml^{-1} in a 1 mg ml^{-1} SiNaPs solution. This corresponds to an average load of 44 peptides per 24 nm SiNaP,

which is only 7% of the theoretical maximal load of 645 peptides, probably as a consequence of repulsive interactions on the nanoparticle surface.

Aβ-SiNaP quantitation in water and cerebrospinal fluid by sFIDA

The sFIDA assay is designed to specifically determine the Aβ oligomer concentration in body fluids, such as cerebrospinal fluid (CSF). Apart from quantifying Aβ-SiNaPs in aqueous environment, we also analyzed possible matrix effects on the sFIDA readout by spiking Aβ-SiNaPs into CSF from AD-negative donors (Fig. 4).

Aβ-SiNaP concentrations ranging from 100 pM to 10 fM were subjected to sFIDA analysis, and the respective non-spiked fluids served as controls. All samples including blank controls were determined three-fold by sFIDA analysis. Aβ-SiNaPs diluted in water as well as in CSF revealed a correlation between the sFIDA readout and the Aβ-SiNaP concentration down to 10 fM. A concentration of 10 fM Aβ-SiNaPs in water and 100 fM in CSF could still be differentiated from the control demonstrating that Aβ-SiNaPs are a suitable standard in CSF-based AD diagnostics.

Considering a load of 44 $A\beta_{42}$ peptides per Aβ-SiNaP, 10 fM Aβ-SiNaP corresponded to an $A\beta_{42}$ peptide concentration of 1.9 ng l^{-1}. This limit of detection of $A\beta_{42}$ peptides is in the same range or one order of magnitude higher as reported for oligomer-specific ELISA-based assays [13, 14, 27]. By repetition of the experiment with the same Aβ-SiNaP batch stored at 4°C over a period of four months, we demonstrated constantly stable sFIDA readouts from the Aβ-SiNaP dilution series and therefore confirmed long-term stability of the standard (Fig. 5).

DISCUSSION

In this work we presented the synthesis and application of Aβ-SiNaPs as standard in sFIDA diagnostics. The successful synthesis and biofunctionalization of SiNaPs was shown by TEM, XPS micrographs and ATR-FTIR spectra. By sFIDA analysis we quantified Aβ-SiNaPs diluted in water and CSF over several orders of magnitude down to the femtomolar concentration range. A SiNaP standard of tunable, defined size and with an adjustable number of epitopes on the SiNaP surface might significantly contribute to the development, optimization and calibration of immuno-based diagnostic

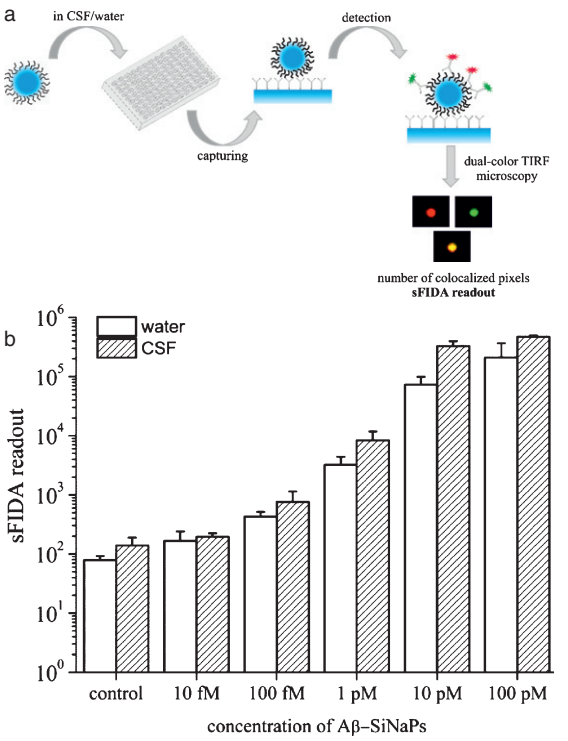

Fig. 4. sFIDA analysis of Aβ-SiNaPs. a) Schematic illustration of the experimental procedure of detecting Aβ-SiNaPs in the sFIDA assay. b) sFIDA analysis of Aβ-SiNaPs diluted in water and CSF sFIDA readout of Aβ-SiNaPs diluted in water and human CSF to concentrations of 100 pM to 10 fM. The respective diluent lacking Aβ-SiNaPs served as negative control. Shown are mean values and standard deviations from threefold determination.

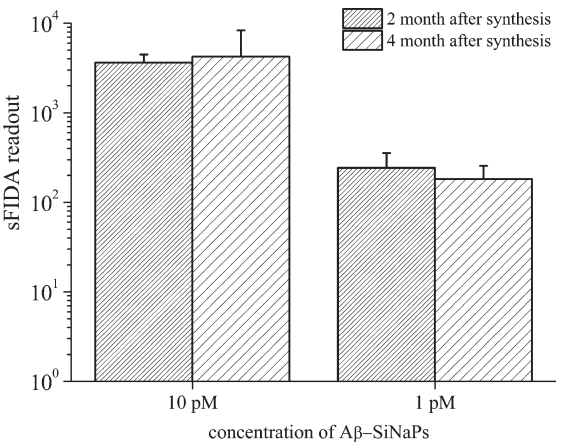

Fig. 5. sFIDA analysis of Aβ-SiNaPs diluted in water. sFIDA readout of Aβ-SiNaPs diluted in water to concentrations of 10 pM and 1 pM. Shown are two measurements of the same SiNaP batch at different time points, 2 and 4 months after synthesis. Plotted are mean values and standard deviations from threefold determination.

assays for protein misfolding diseases based on single-molecule detection.

In contrast to any other standard of Aβ aggregates, Aβ-SiNaPs exhibit a measurable number of accessible Aβ peptides on the SiNaP surface. These defined characteristics render Aβ-SiNaPs superior to the more heterogeneous oligomer standards prepared from a stochastic aggregation reaction of synthetic Aβ, as they have been used so far. In the presented case we bound 44 peptides per SiNaP.

In addition, Aβ-SiNaPs prepared by this method showed no observable aggregation after the excessive and non-covalently bound monomer was removed. This observation suggests that Aβ bound to the particle surface is not able to transmit to a conformation that is prone to form aggregates. Since the mid and C-terminal sections of the Aβ sequence are involved in the aggregation mechanism it appears very likely that the coupling of Lys16 and/or Lys28 is responsible for the inhibition of the aggregation of Aβ-SiNaP.

The chemically activated SiNaPs can be easily coated with any peptide of choice to serve also as standard in oligomer-based assays of other protein misfolding diseases, such as prion diseases or Parkinson's disease [28–31]. Additionally, hybrid aggregates consisting of different peptides, such as tau and Aβ, could be mimicked by a SiNaP standard to support explorative studies on hybrid oligomers as biomarkers, which might reflect the clinical diversity of many neurodegenerative disorders [32, 33]. For the described synthesis of biofunctionalized SiNaPs the chosen peptide needs to have a free primary amine group for the covalent coupling to the SiNaP outside the epitope, to enable detection of the peptide on the SiNaP. Alternatively other coupling methods, such as Biotin/Streptavidin could link peptides to the SiNaP platform.

Different approaches are developed for the oligomer-specific diagnosis of Alzheimer's disease based on immunodetection in liquid, such as ELISA-like methods as described above or flow cytometry combined with FRET [34]. However, these methods lack an appropriate standard molecule to enable the accurate and reproducible quantitation of Aβ oligomers in human samples. A calibration curve of a serial dilution of Aβ-SiNaPs in the respective body fluid should allow the quantitation of the analyte and also the number of detected epitopes by comparing the obtained fluorescence signals of the clinical sample and the standard.

We envisage the Aβ-SiNaP standard as an essential tool to cross-validate Aβ oligomers as AD biomarker on different platform technologies. It will allow the accurate determination of inter-assay variability and thereby be a valuable tool in the standardization process of various Aβ oligomer immunodetection assays.

ACKNOWLEDGMENTS

This work was supported by the Federal Ministry of Education and Research within the projects VIP (03V0641), KNDD (01GI1010A), and JPND/BIOMARKAPD (01ED1203H).

Authors' disclosures available online (http://www.j-alz.com/manuscript-disclosures/16-0253r2).

REFERENCES

[1] Prince M, Albanese E, Guerchet M, Prina M (2014) *World Alzheimer Report 2014, Dementia and Risk Reduction: An Analysis of Protective and Modifiable Factors*.

[2] Barnes DE, Yaffe K (2011) The projected effect of risk factor reduction on Alzheimer's disease prevalence. *Lancet Neurol* **10**, 819-828.

[3] Hardy J, Selkoe DJ (2002) The amyloid hypothesis of Alzheimer's disease: Progress and problems on the road to therapeutics. *Science* **297**, 353-356.

[4] Hardy J (2006) Has the amyloid cascade hypothesis for Alzheimer's disease been proved? *Curr Alzheimer Res* **3**, 71-73.

[5] Haass C, Selkoe DJ (2007) Soluble protein oligomers in neurodegeneration: Lessons from the Alzheimer's amyloid beta-peptide. *Nat Rev Mol Cell Biol* **8**, 101-112.

[6] Lesne S, Koh MT, Kotilinek L, Kayed R, Glabe CG, Yang A, Gallagher M, Ashe KH (2006) A specific amyloid-beta protein assembly in the brain impairs memory. *Nature* **440**, 352-357.

[7] El-Agnaf OM, Mahil DS, Patel BP, Austen BM (2000) Oligomerization and toxicity of beta-amyloid-42 implicated in Alzheimer's disease. *Biochem Biophys Res Commun* **273**, 1003-1007.

[8] Klaver AC, Patrias LM, Finke JM, Loeffler DA (2011) Specificity and sensitivity of the Abeta oligomer ELISA. *J Neurosci Methods* **195**, 249-254.

[9] Savage MJ, Kalinina J, Wolfe A, Tugusheva K, Korn R, Cash-Mason T, Maxwell JW, Hatcher NG, Haugabook SJ, Wu GX, Howell BJ, Renger JJ, Shughrue PJ, McCampbell A (2014) A sensitive A beta oligomer assay discriminates Alzheimer's and aged control cerebrospinal fluid. *J Neurosci* **34**, 2884-2897.

[10] Sian AK, Frears ER, El-Agnaf OM, Patel BP, Manca MF, Siligardi G, Hussain R, Austen BM (2000) Oligomerization of beta-amyloid of the Alzheimer's and the Dutch-cerebral-haemorrhage types. *Biochem J* **349**, 299-308.

[11] Xia W, Yang T, Shankar G, Smith IM, Shen Y, Walsh DM, Selkoe DJ (2009) A specific enzyme-linked immunosorbent assay for measuring beta-amyloid protein oligomers in human plasma and brain tissue of patients with Alzheimer disease. *Arch Neurol* **66**, 190-199.

[12] Yang T, O'Malley TT, Kanmert D, Jerecic J, Zieske LR, Zetterberg H, Hyman BT, Walsh DM, Selkoe DJ (2015) A

highly sensitive novel immunoassay specifically detects low levels of soluble A beta oligomers in human cerebrospinal fluid. *Alzheimers Res Ther* **7**, 14.

[13] Holtta M, Hansson O, Andreasson U, Hertze J, Minthon L, Nagga K, Andreasen N, Zetterberg H, Blennow K (2013) Evaluating amyloid-beta oligomers in cerebrospinal fluid as a biomarker for Alzheimer's disease. *PLoS One* **8**, e66381.

[14] Fukumoto H, Tokuda T, Kasai T, Ishigami N, Hidaka H, Kondo M, Allsop D, Nakagawa M (2010) High-molecular-weight beta-amyloid oligomers are elevated in cerebrospinal fluid of Alzheimer patients. *FASEB J* **24**, 2716-2726.

[15] Funke SA, Birkmann E, Henke F, Goertz P, Lange-Asschenfeldt C, Riesner D, Willbold D (2007) Single particle detection of A beta aggregates associated with Alzheimer's disease. *Biochem Biophys Res Commun* **364**, 902-907.

[16] Wang-Dietrich L, Funke SA, Kuhbach K, Wang K, Besmehn A, Willbold S, Cinar Y, Bannach O, Birkmann E, Willbold D (2013) The amyloid-beta oligomer count in cerebrospinal fluid is a biomarker for Alzheimer's disease. *J Alzheimers Dis* **34**, 985-994.

[17] Mattsson N, Andreasson U, Persson S, Carrillo MC, Collins S, Chalbot S, Cutler N, Dufour-Rainfray D, Fagan AM, Heegaard NH, Robin Hsiung GY, Hyman B, Iqbal K, Kaeser SA, Lachno DR, Lleo A, Lewczuk P, Molinuevo JL, Parchi P, Regeniter A, Rissman RA, Rosenmann H, Sancesario G, Schroder J, Shaw LM, Teunissen CE, Trojanowski JQ, Vanderstichele H, Vandijck M, Verbeek MM, Zetterberg H, Blennow K, Alzheimer's Association QCPWG (2013) CSF biomarker variability in the Alzheimer's Association quality control program. *Alzheimers Dement* **9**, 251-261.

[18] Stober W, Fink A, Bohn E (1968) Controlled growth of monodisperse silica spheres in micron size range. *J Colloid Interface Sci* **26**, 62-69.

[19] Thomassen LC, Aerts A, Rabolli V, Lison D, Gonzalez L, Kirsch-Volders M, Napierska D, Hoet PH, Kirschhock CE, Martens JA (2010) Synthesis and characterization of stable monodisperse silica nanoparticle sols for *in vitro* cytotoxicity testing. *Langmuir* **26**, 328-335.

[20] Glabe CG (2008) Structural classification of toxic amyloid oligomers. *J Biol Chem* **283**, 29639-29643.

[21] Mastrangelo IA, Ahmed M, Sato T, Liu W, Wang C, Hough P, Smith SO (2006) High-resolution atomic force microscopy of soluble Abeta42 oligomers. *J Mol Biol* **358**, 106-119.

[22] Sakono M, Zako T (2010) Amyloid oligomers: Formation and toxicity of Abeta oligomers. *FEBS J* **277**, 1348-1358.

[23] Masalov VM, Sukhinina NS, Kudrenko EA, Emelchenko GA (2011) Mechanism of formation and nanostructure of Stober silica particles. *Nanotechnology* **22**, 275718.

[24] Graf C, van Blaaderen A (2002) Metallodielectric colloidal core-shell particles for photonic applications. *Langmuir* **18**, 524-534.

[25] Nag S, Chen J, Irudayaraj J, Maiti S (2010) Measurement of the attachment and assembly of small amyloid-beta oligomers on live cell membranes at physiological concentrations using single-molecule tools. *Biophys J* **99**, 1969-1975.

[26] Qhobosheane M, Santra S, Zhang P, Tan W (2001) Biochemically functionalized silica nanoparticles. *Analyst* **126**, 1274-1278.

[27] Bruggink KA, Jongbloed W, Biemans EA, Veerhuis R, Claassen JA, Kuiperij HB, Verbeek MM (2013) Amyloid-beta oligomer detection by ELISA in cerebrospinal fluid and brain tissue. *Anal Biochem* **433**, 112-120.

[28] Bannach O, Birkmann E, Reinartz E, Jaeger KE, Langeveld JP, Rohwer RG, Gregori L, Terry LA, Willbold D, Riesner D (2012) Detection of prion protein particles in blood plasma of scrapie infected sheep. *PLoS One* **7**, e36620.

[29] Bannach O, Reinartz E, Henke F, Dressen F, Oelschlegel A, Kaatz M, Groschup MH, Willbold D, Riesner D, Birkmann E (2013) Analysis of prion protein aggregates in blood and brain from pre-clinical and clinical BSE cases. *Vet Microbiol* **166**, 102-108.

[30] Hubinger S, Bannach O, Funke SA, Willbold D, Birkmann E (2012) Detection of alpha-synuclein aggregates by fluorescence microscopy. *Rejuvenation Res* **15**, 213-216.

[31] Hansson O, Hall S, Ohrfelt A, Zetterberg H, Blennow K, Minthon L, Nagga K, Londos E, Varghese S, Majbour NK, Al-Hayani A, El-Agnaf OM (2014) Levels of cerebrospinal fluid alpha-synuclein oligomers are increased in Parkinson's disease with dementia and dementia with Lewy bodies compared to Alzheimer's disease. *Alzheimers Res Ther* **6**, 25.

[32] Clinton LK, Blurton-Jones M, Myczek K, Trojanowski JQ, LaFerla FM (2010) Synergistic Interactions between Abeta, tau, and alpha-synuclein: Acceleration of neuropathology and cognitive decline. *J Neurosci* **30**, 7281-7289.

[33] Guo JP, Arai T, Miklossy J, McGeer PL (2006) A beta and tau form soluble complexes that may promote self aggregation of both into the insoluble forms observed in Alzheimer's disease. *Proc Natl Acad Sci U S A* **103**, 1953-1958.

[34] Santos AN, Torkler S, Nowak D, Schlittig C, Goerdes M, Lauber T, Trischmann L, Schaupp M, Penz M, Tiller FW, Bohm G (2007) Detection of amyloid-beta oligomers in human cerebrospinal fluid by flow cytometry and fluorescence resonance energy transfer. *J Alzheimers Dis* **11**, 117-125.